ELSEVIER

Thermochimica Acta 389 (2002) 79–83

thermochimica acta

www.elsevier.com/locate/tca

Study on the kinetics of thermal decomposition of mechanically activated pyrites

Huiping Hu*, Qiyuan Chen, Zhoulan Yin, Pingmin Zhang, Jianpeng Zou, Hongsheng Che

College of Chemistry and Chemical Engineering, Central South University, Changsha 410083, PR China

Received 16 July 2001; received in revised form 19 November 2001; accepted 19 November 2001

Abstract

The kinetics of the thermal decompositions of mechanically activated pyrite and non-activated pyrite was studied by using Friedman method at different heating rates of 2.5, 5, 7.5 and 15 K min^{-1} in argon. Results show that the activation energies (E), reaction orders (n) and pre-exponential factors (A) are 268.612 kJ mol^{-1}, 0.42 and 1.094×10^{15} min^{-1} for non-activated pyrite, 243.725 kJ mol^{-1}, 0.62 and 2.008×10^{13} min^{-1} for pyrite mechanically activated for 20 min (abbreviated as activated pyrite 1, 177.288 kJ mol^{-1}, 0.65 and 5.924×10^{9} min^{-1} for pyrite mechanically activated for 40 min (abbreviated as activated pyrite 2, respectively. Comparing the integral width of X-ray diffraction peaks (220) and (440) of activated pyrites at different grinding time with that of non-activated pyrite, several values of the deformation (ε) of crystal lattice and the particle size (D) of the crystallite were obtained. It is found that the mechanical activation of the original material brings about a change in surface structure of pyrite, which results in non-activated pyrite's transformation into metastable pyrite in the course of mechanical activation. The metastable pyrite is more liable to thermal decomposition than non-activated pyrite.

Keywords: TG–DTG measurement; Mechanical activation; Pyrite; Thermal decomposition; Activation energy

1. Introduction

Gold deposits can be broadly classified into two categories, primary and secondary. The primary deposits are sulfides, mainly pyrite and arsenopyrite. Direct leaching of the secondary deposits give good gold recoveries, but direct leaching of the primary deposits give poor recoveries, depending on the mineralogical composition of the deposit and the form of the gold in the host. The difficult-to-treat concentrates, such as pyrite and arsenopyrite, are described as refractory [1]. It has been known for some time that the reactivity of minerals can be improved by grinding—a process known as 'mechanical activation'. For example ultrafine grinding of chalcopyrite increases its activity so that less severe leaching conditions are required to recover the copper [2,3]. Thus, the term mechanical activation refers to mechanically induced enhancement of the chemical reactivity of a system [4]. In the past 10 years, a more focused effort has been made to qualify the kinetic enhancements due to mechanical activation, which are attributed to the increased specific surface area, enhanced surface reactivity, and changes in the crystalline structure (e.g. amorphization) [5–9]. The commonly used methods

* Corresponding author.
E-mail address: hhuiping@mail.csu.edu.cn (H. Hu).

0040-6031/02/$ – see front matter
PII: S0040-6031(01)00850-4

[10–12] to identify changes in surfaces, structural and spectroscopic properties, and other properties are BET, scanning electron microscopy, X-ray photoelectron (XPS), infrared, X-ray diffraction, Mössbauer spectroscopy, electron spin resonance (ESR), DTA and DSC, etc. But few concerns have been made on the thermal stability of mechanically activated pyrite, especially on the kinetics of thermal decomposition of mechanically activated pyrite.

In this paper, two kinds of mechanically activated pyrites after grinding the natural pyrite for 20 and 40 min, abbreviated as activated pyrite 1 and activated pyrite 2, respectively, were obtained. The kinetic study of non-isothermal decomposition processes of these pyrites under a dynamic argon atmosphere has been studied using the TG–DTG technique. The activation energies (E), reaction order (n) and pre-exponential factor (A) for different pyrites are presented. The results were compared with the changes of the surface structures of different pyrites after mechanical activation.

2. Experimental

Natural pyrite ore was purchased from a domestic geological museum, and its chemical compositions are presented in Table 1. It was found by X-ray diffraction analysis that the natural pyrite contained cubic pyrite as a predominant component. The non-activated pyrite was prepared by crushing the natural pyrite in a jaw crusher to a particle size of $\leq$1 mm, then stored for more than 1 year. The non-activated pyrite (10 g) was mechanically activated in a planetary mill (QM-ISP Planetary mill, PR China) with six stainless steel balls of 18 mm in diameter and 12 balls of 8 mm in diameter under a rotation rate of 200 rpm. A powder-to-ball mass ratio of 1:25 was employed. The pyrite powder samples were milled in air for 20 and 40 min to get two kinds of mechanically activated pyrites abbreviated as activated pyrites 1 and 2, respectively.

The structure disorder of mechanically activated pyrites was determined by X-ray diffraction analysis on the diffractometer (3014 Rigaku, Japan) using Cu Kα radiation ($\lambda = 1.54$ Å, voltage 40 kV, current 20 mA) with time constant 0.5 s, limit of measurement 10 impulses S^{-1}, scanning speed $2^\circ\,min^{-1}$. The degree of structural disorder was evaluated from the deformation (ε) of crystal lattice (presented as a percentage). The decrease of the particle size (D) of the crystallite (presented as the particle dimension of the crystallite) was also observed, which was determined from the changes in profile of the diffraction peaks, such as (220) and (440) of pyrite. From the theoretical analysis of diffraction peaks, the breadth of diffraction peaks mainly result from the increase of the deformation (ε) of crystal lattice and the decrease of the particle size (D) of the crystallite, ε and D were calculated using the model of Gaussian function [13].

The measurements pertaining to thermogravimetry were performed by using a thermal analyzer TGA/SDTA 851^e (Mettler Toledo, USA and Switzerland) with a temperature program from 25–1000 °C at the heating rates of 2.5, 5, 7.5 and 15 K min^{-1} in argon, respectively. The sample mass is 34 mg.

The specific granulometric surface area, S_G, of activated pyrites was calculated from the corresponding average particle size measured using Mastersizer 2000 Laser Diffraction Particle Size Analyzer (Malvern, Great Britain), distilled water was used as a dispersing agent in the experiments.

3. Theoretical analysis

A commonly used form for thermal decomposition of a solid can be expressed as Eq. (1):

$$-\frac{dw}{dt} = kf(w) \tag{1}$$

where w is the remaining weight of the sample at a certain time, which is defined as $w = w_t - w_\infty$, in which w_t and w_∞ are the weights of the sample during

Table 1
The chemical analyses of the natural pyrite

Elements	Fe	S	Si	Ca	Sn	Sb	As	Zn	Co	Ni
Content (wt.%)	45.63	52.38	0.1	0.01	0.01	0.01	0.03	0.05	0.005	0.001

the reaction at t and t_∞, respectively. At a certain heating rate $\beta_i = dT/dt = \text{constant}$, we have Eq. (2)

$$-\frac{dw}{dt} = \frac{A}{\beta_i} e^{-E/RT} f(w) \quad (2)$$

where A, E, T and R are pre-exponential factor, activation energy, temperature and gas constant. Because of the strong mutual interdependence of parameters E and A in Eq. (2), it has been suggested that the so-called multiple-scan methods available [14,15] be applied for calculation of the activation energy from several sets of kinetic data taken at various heating rates. In the present study, the Friedman method was used to obtain E value according to Eq. (3)

$$\ln\left[\beta_i\left(-\frac{dw}{dt}\right)\right] = \ln[Af(w)] - \frac{E}{RT} \quad (3)$$

For a given w, we have a series of T values from different TG curves at different heating rates β_i. Plotting $\ln[\beta_i(dw/dt)]$ versus $1/T$ at different w, several slopes ($-E/R$) and intercepts ($\ln[Af(w)]$) can be obtained from the curves. The n and A can be obtained from Eq. (4).

$$\ln[Af(w)] = \ln A + n \ln w \quad (4)$$

4. Results and discussion

4.1. TG curves for different pyrites

The TG curves for different pyrites were obtained at the heating rates of 2.5, 5.0, 7.5 and 15 K min^{-1}, respectively (Figs. 1–3).

4.2. The Friedman method for different pyrites at multi-heating rates

A group of paralleled lines of plotting $\ln[\beta_i(-dw/dt)]$ versus $1/T$ were obtained for non-activated pyrite at $w = 4.3$, 3.5, 2.5 and 2.3 mg, for activated pyrite 1 at $w = 3.8$, 3.3, 2.6 and 2.3 mg, and for activated pyrite 2 at $w = 4.3$, 3.3, 2.6 and 2.1 mg, which are shown in Figs. 4–6, respectively.

The activation energy (E) can be obtained from the slope of the regression line. Plotting intercept $\ln[Af(w)]$ versus $\ln w$, n and A can be calculated. All the results are listed in Table 2.

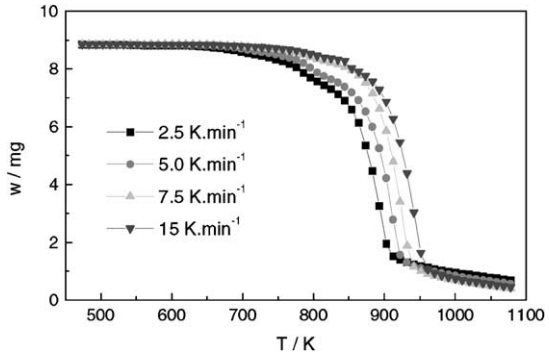

Fig. 1. TG curves for non-activated pyrite at different heating rates.

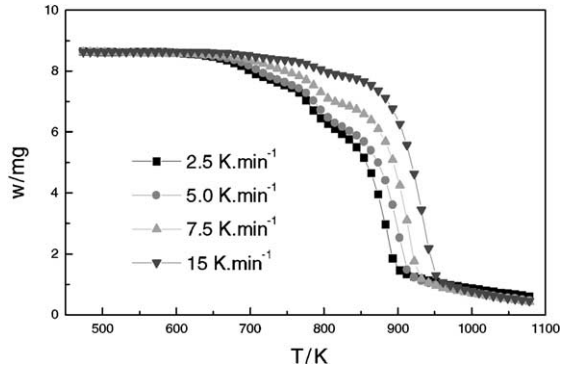

Fig. 2. TG curves for activated pyrite 1 at different heating rates.

From Table 2, it is found that the activation energies of the thermal decomposition of the samples decreased gradually in the order of non-activated pyrite, activated pyrite 1 and activated pyrite 2. The state of the activated solids can be characterized as

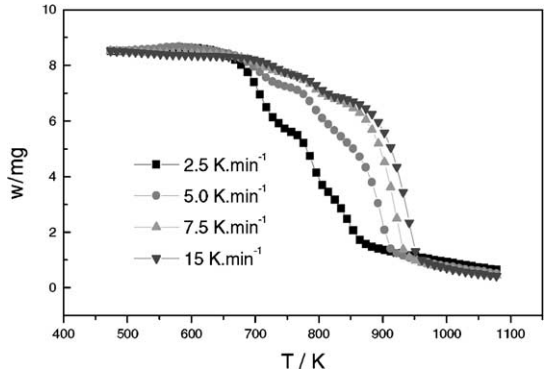

Fig. 3. TG curves for activated pyrite 2 at different heating rates.

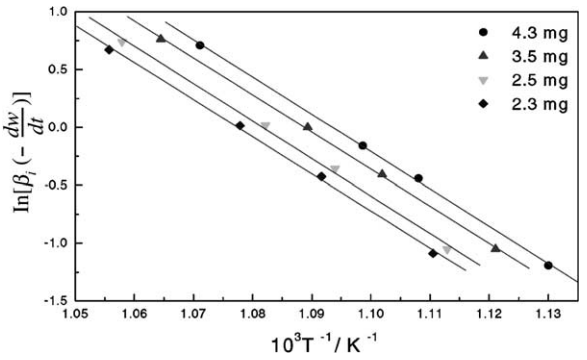

Fig. 4. Plots of $\ln[\beta_i(-\mathrm{d}w/\mathrm{d}t)]$ vs. $1/T$ for non-activated pyrite at different w.

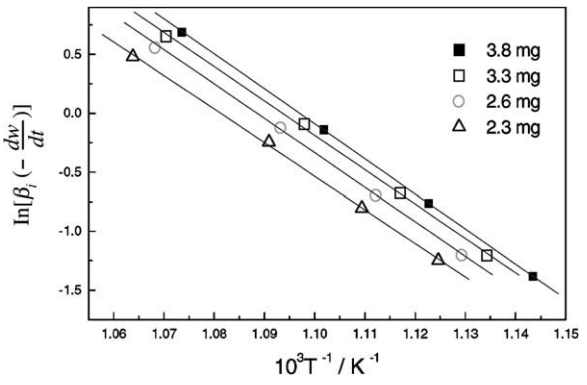

Fig. 5. Plots of $\ln[\beta_i(-\mathrm{d}w/\mathrm{d}t)]$ vs. $1/T$ for activated pyrite 1 at different w.

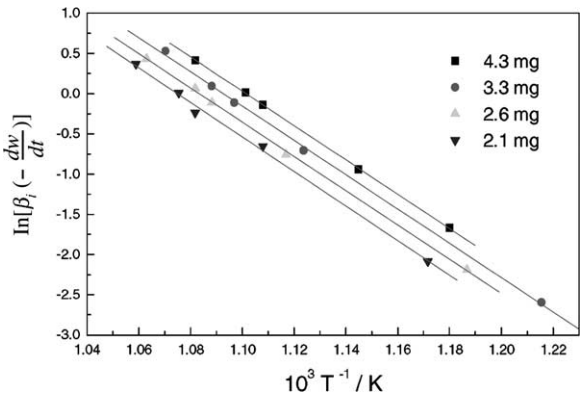

Fig. 6. Plot of $\ln[\beta_i(-\mathrm{d}w/\mathrm{d}t)]$ vs. $1/T$ for activated pyrite 2 at different w value.

Table 2
E, A and n of non-activated pyrite, activated pyrite 1 and activated pyrite 2

Samples	E (kJ mol^{-1})	A (min^{-1})	n
Non-activated pyrite	268.612	1.094×10^{15}	0.42
Activated pyrite 1	243.725	2.008×10^{13}	0.62
Activated pyrite 2	177.288	5.924×10^{9}	0.65

metastable [16] and non-activated pyrite transforms into metastable pyrites [17] after mechanical activation. This metastable pyrite is more liable to thermal decomposition than non-activated pyrite because the activation energies of the thermal decomposition of the samples decreases gradually with increasing grinding time, which coincides with thermoanalytical study of mechanically activated cinnabar by Baláź [12].

4.3. Study on the changes of surface structure of activated pyrites

By analyzing the integral width of X-ray diffraction peaks (220) and (440) of non-activated pyrite and activated pyrites, the values of D and ε are listed in Table 3.

Table 3 shows that the particle size of the crystal lattice decreased and the deformation of the crystal structure increased gradually with increasing grinding time, which is in agreement with the study of mechanically activated chalcopyrite [18]. And the increase of effective Debye–Waller parameters of $B_{\mathrm{eff}}(\mathrm{FeS_2})$ for the overall crystal and $B_{\mathrm{eff}}(\mathrm{S})$ for sulfur with increasing grinding time for pyrites provides additional insight into the mechanisms of the structural disordering process upon milling [19].

The specific granulometric surface area, S_{G}, is shown in Table 4, the surface area increases with grinding.

Eymery and Ylli [17] have reported a phase transformation from pyrite $\mathrm{FeS_2}$ ($\mathrm{Fe^{2+}}$ in a low-spin state)

Table 3
The relationship between D, ε and grinding time t

	t (min)			
	10	20	30	40
D (Å)	3932	2988	1166	675
ε (%)	0.02	0.03	0.05	0.06

Table 4
The specific granulometric surface area, S_G, vs. the grinding time t

	t (min)				
	10	20	30	40	60
S_G ($m^2\ g^{-1}$)	15.3245	18.2234	18.2211	18.2677	20.0521

to szomolnokite $FeSO_4{\cdot}H_2O$ (Fe^{2+} in a high-spin state) during the mechanical activation of ball milling in air, which was observed by using ^{57}Fe Mössbauer spectroscopy. And the contents of szomolnokite $FeSO_4{\cdot}H_2O$ becomes larger with increasing milling time. Zou [20] investigated the mechanical activation of pyrites by ball milling in air by XPS, and found that not only the disulfidic form (S_2^{2-}) but also the sulfate form also occurs in the mechanically activated pyrites.

Therefore, non-activated pyrite undergoes mechanochemical reaction, the increase of the surface area and the structural distortion during grinding in air, which leads to the formation of metastable pyrites. The metastable pyrites containing accumulated excess energy can thermally decompose more easily than non-activated pyrites. This structural sensitivity of thermal decomposition of these pyrites also confirms the structural sensitivity of thermal decomposition of mechanically activated chalcopyrite and sphalerite [16,21].

5. Conclusions

The activation energies, reaction orders and pre-exponential factors of the thermal decompositions of mechanically activated pyrites and non-activated pyrites are calculated according to Friedman method at different heating rates. The change in the surface structure of pyrite during mechanical activation is also studied and mechanical activation results in non-activated pyrite's transformation into metastable pyrite, which is more liable to thermal decomposition than non-activated pyrite.

Acknowledgements

This investigation is supported by the National Key Project of Natural Science Foundation in PR China.

References

[1] M.N. Lehmann, S.O. Leary, J.G. Dunn, Miner. Eng. 13 (1) (2000) 1.
[2] I.J. Corrans, J.E. Angove, Miner. Eng. 4 (711) (1991) 763.
[3] C.J. Warris, P.G. McCormick, Miner. Eng. 10 (10) (1997) 1119.
[4] K. Tkácová, P. Baláz, Int. J. Miner. Process 44/45 (1996) 197.
[5] P. Baláz, I. Ebert, Hydrometallury 27 (1991) 141.
[6] K. Tkácová, P. Baláz, Hydrometallurgy 21 (1988) 103.
[7] K. Tkácová, P. Baláz, B. Mišura, V.E. Vigdergauz, V.A. Chanturiya, Hydrometallurgy 33 (1993) 291.
[8] P. Baláz, J. Bruancin, V. Šepelák, T. Havlík, M. Škrobian, Hydrometallurgy 31 (1992) 201.
[9] L.E. Murr, J.B. Hskey, Met. Trans. B 12B (1981) 255.
[10] P. Baláz, Hydrometallurgy 40 (1996) 359.
[11] P. Baláz, Z. Bastl, J. Bruancin et al., J. Mater. Sci. 27 (1992) 653.
[12] P. Baláz, E. Post, Z. Bastl, Thermochim. Acta 200 (7–8) (1992) 371.
[13] Shixiong Sheng, Technology of X-ray diffraction, Metallurgy Industrial Press, 1986 (in Chinese).
[14] L. Reich, W. Levi, in: Macromolecular Review, Vol. 1, Wiley-Interscience, New York, 173, 1986.
[15] H.L. Friedman, J. Macromol. Sci. (Chem.) 41 (1967) 57.
[16] V.V. Boldyrev, Proc. Indian Nat. Sci. Acad., Part A 52 (1986) 400.
[17] J.P. Eymery, F. Ylli, J. Alloys Compounds 298 (2000) 306.
[18] L. Honggui, Y. Jiahong, Z. Zhongwei, J. Centr. South Univ. Tech. 29 (1) (1998) 28 (in Chinese).
[19] K. Sasak, H. Konno, M. Inagaki, J. Mater. Sci. 29 (1994) 1666.
[20] Jianpeng Zou, Academic Thesis for postgraduate, 1999 (in Chinese).
[21] P. Baláz, I. Ebert, Thermochim. Acta 180 (1991) 117.